UDC 669.295:669.018.9
https://doi.org/10.17073/0021-3438-2023-6-54-65

Research article
Научная статья

Influence of partial titanium substitution by its hydride on structure and mechanical properties of TNM-B1 heat-resistant alloy, obtained by SHS powder hot isostatic pressing

G.M. Markov[1], **P.A. Loginov**[1], **N.V. Shvyndina**[1], **F.A. Baskov**[1,2], **E.A. Levashov**[1]

[1] **National University of Science and Technology "MISIS"**
4 build. 1 Leninskiy Prosp., Moscow 119049, Russia

[2] **JSC "Composite"**
4 Pionerskaya Str., Moscow region, Korolev 141074, Russia

✉ Georgy M. Markov (markov.sci@gmail.com)

Abstract: This paper investigates the influence of partial substitution of titanium by its hydride on the microstructure and mechanical properties of TNM-B1 alloy obtained by powder metallurgy technology. The impact of the Ti:TiH_2 ratio in the reaction mixture and heat treatment modes on the microstructure and mechanical properties of TNM-B1+1%Y_2O_3 alloy, obtained using high-energy ball milling (HEBM), self-propagating high-temperature synthesis (SHS), and hot isostatic pressing (HIP) methods, has been examined. It was observed that a 10 % substitution of titanium with its hydride in the reaction mixtures reduces the oxygen content in SHS products from 1 % to 0.8 % due to the generation of a reducing atmosphere during the decomposition of TiH_2 in the combustion wave. When the Ti : TiH_2 ratio is 90 : 10, highest mechanical properties of TNM-B1+1%Y_2O_3 alloy were achieved: a compressive strength (σ_u) of 1200±15 MPa and a yield strength (YS) of 1030±25 MPa. An increase in the proportion of TiH_2 results in a higher content of oxygen impurity, leading to the formation of Al_2O_3, which reduces the strength and ductility of the material. With additional heat treatment of TNM-B1+1%Y_2O_3 alloy, the globular structure transforms into a partially lamellar one, leading to an increase in σ_u by 50–300 MPa, depending on the TiH_2 content. This attributed to a decrease in the average grain size and a reduction in dislocation mobility during deformation.

Keywords: titanium alloys, titanium hydride, powder metallurgy, high energy machining (HEBM), self-propagating high temperature synthesis (SHS), hot isostatic pressing (HIP), mechanical properties.

Acknowledgments: This work received support from the Ministry of Science and Higher Education of the Russian Federation (Project No. 0718-2020-0034).

For citation: Markov G.M., Loginov P.A., Shvyndina N.V., Baskov F.A., Levashov E.A. Influence of partial titanium substitution by its hydride on structure and mechanical properties of TNM-B1 heat-resistant alloy, obtained by SHS powder hot isostatic pressing. *Izvestiya. Non-Ferrous Metallurgy*. 2023;29(6):54–65.
https://doi.org/10.17073/0021-3438-2023-6-54-65

Влияние частичного замещения титана его гидридом на структуру и свойства жаропрочного сплава TNM-B1, полученного методом горячего изостатического прессования СВС-порошка

Г.М. Марков[1], **П.А. Логинов**[1], **Н.В. Швындина**[1], **Ф.А. Басков**[1,2], **Е.А. Левашов**[1]

[1] **Национальный исследовательский технологический университет «МИСИС»**
Россия, 119049, г. Москва, Ленинский пр-т, 4, стр. 1

[2] **АО «Композит»**
Россия, 141074, Московская обл., г. Королев, ул. Пионерская, 4

✉ Георгий Михайлович Марков (markov.sci@gmail.com)

Аннотация: В работе исследовано влияние частичного замещения титана его гидридом на микроструктуру и механические свойства сплава TNM-B1, полученного по технологии порошковой металлургии. Рассмотрено влияние соотношения Ti:TiH_2 в реакционной смеси и режимов термообработки на микроструктуру и механические свойства сплава TNM-B1+1%Y_2O_3, полученного с использованием методов высокоэнергетической механической обработки (ВЭМО), самораспространяющегося высокотемпературного синтеза (СВС) и горячего изостатического прессования (ГИП). Установлено, что 10 %-ное замещение титана его гидридом в реакционных смесях позволяет уменьшить содержание кислорода в СВС-продуктах с 1 до 0,8 % благодаря созданию восстановительной атмосферы при разложении TiH_2 в волне горения. При соотношении Ti : TiH_2 = = 90 : 10 достигнуты максимальные механические свойства сплава TNM-B1+1%Y_2O_3: прочность при сжатии $\sigma_в$ = 1200±15 МПа и предел текучести $\sigma_{0,2}$ = 1030±25 МПа. Рост доли TiH_2 увеличивает содержание примесного кислорода, приводящего к образованию Al_2O_3, который снижает прочность и пластичность материала. За счет дополнительной термообработки сплава TNM-B1+1%Y_2O_3 глобулярная структура преобразуется в частично ламеллярную, что приводит к увеличению $\sigma_в$ на 50–300 МПа в зависимости от содержания TiH_2. Получаемый эффект обусловлен уменьшением среднего размера зерен и снижением подвижности дислокаций при деформации.

Ключевые слова: титановые сплавы, гидрид титана, порошковая металлургия, высокоэнергетическая механическая обработка (ВЭМО), самораспространяющийся высокотемпературный синтез (СВС), горячее изостатическое прессование (ГИП), механические свойства.

Благодарности: Работа выполнена при финансовой поддержке Министерства науки и высшего образования РФ в рамках государственного задания (проект 0718-2020-0034).

Для цитирования: Марков Г.М., Логинов П.А., Швындина Н.В., Басков Ф.А., Левашов Е.А. Влияние частичного замещения титана его гидридом на структуру и свойства жаропрочного сплава TNM-B1, полученного методом горячего изостатического прессования СВС-порошка. *Известия вузов. Цветная металлургия.* 2023;29(6):54–65.
https://doi.org/10.17073/0021-3438-2023-6-54-65

Introduction

Heat-resistant alloys based on TiAl/Ti3Al intermetallic compounds represent an independent class of materials, the main feature of which is high strength at elevated temperatures and heat resistance. These alloys find applications in the field of engine construction, where materials capable of enduring high-temperature loads for extended periods are essential [1]. Their relatively low density (3.9—4.2 g/cm^3) results in higher specific strength when compared to nickel superalloys. Combined with exceptional creep resistance, this makes them promising candidates for use as materials in low-pressure turbine blades [2; 3].

Most industrial alloys based on TiAl/Ti_3Al contain between 43 to 48 atomic percent aluminum. The optimal aluminum concentration depends on the presence of dopants that influence the position of the γ and α + γ phase regions on the Ti—Al phase diagram. Several generations of alloys based on titanium aluminides have been developed [4]. The 1st generation includes the Ti—48Al—2Cr—2Nb alloy, known as GE4822, as well

as low-alloy analogues like Ti—47Al—2Cr—2Nb and Ti—48Al—2Cr—2Mn [4; 5]. The complexity of the alloying system using V, Zr, W, Ta, Mn, and other elements has led to the creation of 2nd generation alloys [6]. The 3rd generation alloys represent the most advanced materials within the TiAl-based family. They are characterized by a high content of niobium, molybdenum, and the presence of boron, with the primary structural component consisting of $\alpha_2 + \gamma$ eutectoid colonies [7; 8].

Conventional methods for producing intermetallic alloys based on TiAl include casting technologies, such as vacuum induction melting [9]. These methods compete with powder metallurgy techniques [10], which encompass additive manufacturing allowing the production of items with complex geometries from powder [11]. Additionally, a combination of methods involving high-energy ball milling (HEBM) of elemental powder mixtures, self-propagating high-temperature synthesis (SHS), and hot isostatic pressing (HIP) [12—14] are utilized [12—14]. The key advantages of the latter approach are the ability to produce materials with a homogeneous, fine-grained structure and the suppression of the β phase formation, which is characteristic of high-niobium alloys. A non-uniform distribution of the β phase reduces creep resistance and high-temperature strength [15].

In multicomponent alloys, the distribution of elements can be uneven due to their low solubility. The use of HEBM can address this issue by enhancing the uniformity of the element distribution in the reaction mixture, as well as increasing the reactivity of the charge, which positively impacts the degree of conversion during SHS [14].

The SHS process can be implemented in the layer-by-layer combustion mode, resulting from local thermal initiation [16; 17], or in the mode of volumetric combustion (thermal explosion) [6]. This method is widely employed for obtaining intermetallic materials, including titanium aluminides [13; 18].

Challenges in the production of intermetallic alloys through powder metallurgy methods include an increased content of impurity oxygen and microstructural heterogeneity, leading to a decrease in high-temperature strength characteristics [19; 20]. One solution to this issue could be the partial substitution of metallic titanium in the powder reaction mixture with its hydride (TiH_2). TiH_2 is easily ground in a planetary centrifugal mill due to its high brittleness [19], uniformly distributed as individual particles that are insoluble in the matrix [20], and decomposes to metallic titanium at relatively low temperatures (400—750 °C) [21]. TiAl-based alloys with TiH_2 are not produced using conventional casting technology because titanium hydride promotes active pore formation during decomposition and the release of accompanying gases. However, in powder technology, due to the staged nature and flexibility of consolidation modes, the use of TiH_2 is of interest. In this case, it is important to determine the optimal Ti : TiH_2 ratio in the reaction mixture, considering the composition of oxygen impurities, microstructure, and mechanical properties of consolidated and heat-treated samples.

The objective of this research was to study the effect of partial substitution of titanium with its hydride on the microstructure and mechanical properties of the TNM-B1 powder alloy.

Materials and methods

Initial materials

The following powder materials, produced in Russia, were used in this study:

- titanium grade PTOM-1 (AO Polema, particle size $d = 40$ μm);
- TiH_2 powder obtained through the hydrogenation of titanium sponge (ZAO "Plasmoterm", $d \sim 12$ μm);
- aluminum PA-4 (AO "Polema", $d \sim 10$ μm);
- niobium NbP-3a (OOO "GK SMM", $d < 40$ μm);
- molybdenum PM-99.95 (AO "Polema", $d = 5$ μm);
- boron grade V-99A (OOO "NPK Ermakhim", $d \sim 0.2$ μm);
- yttrium oxide nanopowder (ZAO "Plazmoterm", $d \sim 20 \div 100$ nm).

These components were combined in the necessary ratios to produce the well-known 3rd generation TNM-B1 alloy based on TiAl [13, 14], hereafter referred to as TNM-B1+1%Y_2O_3 in the text. The Ti : TiH_2 ratio in the mixture was varied as follows (wt.%): 90 : 10, 80 : 20, 70 : 30, and 60 : 40.

High-energy ball milling

Powder mixtures were prepared in two stages. In the first stage, Ti, TiH_2, Nb, Mo, B, and Y_2O_3 powders were mixed in an Activator-4M planetary centrifugal mill (PCM) (OOO "Machine Building Plant Activator", Russia). The grinding jars were rolled at a speed of 694 rpm for a duration of 10 min. The weight ratio of materials to grinding media was 1 : 15, and the jars were filled with argon to protect the mixture against oxidation. Subsequently, aluminum was added to the Ti/TiH_2–Nb–Mo–B–Y_2O_3 alloy obtained after HEBM, and it was mixed using a rotating ball mill for 2 h. The weight ratio of the mixture components to grind-

ing media was 1 : 10. The use of this mixer in the second stage was necessary to prevent oxidation and the adhesion of plastic aluminum to the jar walls and grinding media.

Self-propagating high-temperature synthesis

Briquetted powder mixtures, following HEBM, were inserted into a tube furnace by advancing crucible with briquettes into a hot zone heated to 900 °C to initiate the SHS process in thermal explosion mode within an argon atmosphere. Following SHS, annealing was conducted in a furnace for 30 min at the same temperature to homogenize the chemical composition of the synthesis products. Subsequent to sintering, the SHS workpieces were crushed using a jaw crusher and a PCM to achieve a powder with a particle size of less than 100 μm. The desired fraction was then separated using sieve classification.

Hot isostatic pressing

The resulting powder was consolidated by the HIP method using an HIRP10/26—200 gas static extruder (ABRA AG, Switzerland). Pre-forming workpieces, which were cylindrical titanium capsules, were annealed in a vacuum at a temperature of 1030 °C for 1 hour to eliminate gas impurities. The HIP process was conducted at 1250 °C and a pressure of 160 MPa, with argon serving as the pressure transfer medium. For the samples consolidated via the HIP method, a heat treatment (HT) was carried out for 2 h at a temperature of 1380 °C in a Termionik T1 vacuum furnace (OOO "Termionika", Russia).

Research procedures for structure and mechanical properties

Powder materials and compact samples were subjected to *X*-ray diffraction analysis (XRD) using a D2 PHASER diffractometer (Bruker AXS GmbH, Germany). CuK_α radiation was employed in the diffraction angle range of $2\theta = 20°\div100°$, with an exposure time of 0.6 s.

The microstructure of both powder and consolidated samples was examined using an S-3400 N scanning electron microscope (Hitachi, Japan), equipped with a NORAN attachment for energy dispersive *X*-ray spectroscopy (EDX). The oxygen content in the mixtures following each technological operation was determined by incinerating the material in an inert atmosphere using a TC-600 device (Leco, USA), in accordance with ASTM E1019-18. Mechanical tests were conducted using uniaxial compression on cylindrical samples ($\varnothing 6 \times 9.0$ mm) with a strain rate of ~0.001 s^{-1}. These tests were performed on an LF-100 kN universal testing machine (Walter + Bai AG, Switzerland).

Results and discussion

High-energy ball milling

Figure 1 illustrates the microstructures of powders with different Ti : TiH_2 ratios obtained using the HEBM method. The base of powder agglomerates, formed during processing due to intense plastic deformation, consists of titanium and its hydride. The primary components are arranged in the form of alternating layers, up to 3 μm thick (Fig. 1, *e*). As the TiH_2 content increases, the degree of their agglomeration into larger particles also increases. The dopants, Nb, and Mo, are uniformly distributed inside the particles in the form of thin layers. This distribution enhances their dissolution rate within the γ-TiAl/α_2-Ti_3Al-based matrix during the SHS process [13].

In the *X*-ray diffraction patterns obtained from the ligature immediately after HEBM, only peaks corresponding to the initial powder materials, including α-Ti, TiH_2, Nb, and Mo, are evident (Fig. 2). The intensity of the TiH_2 peaks increases in proportion to the fraction of hydride in the master alloy, indicating that it remains intact during the HEBM process and does not decompose into metallic titanium and hydrogen. Niobium and molybdenum, characterized by a BCC lattice with an *Im*3*m* space group, are observed in granular form as independent phases. This can be attributed to the low solubility of these components in titanium, which has an HCP lattice, owing to differences in crystal structure as well as their high hardness and low plasticity.

Study of synthesis products and their consolidation via hot isostatic pressing

After further mixing of Ti/TiH2—Nb—Mo—B—Y_2O_3 master alloys with aluminum and conducting syntheses in thermal explosion mode, SHS-sintered samples were obtained, and their microstructure and phase composition were examined. It was observed that the samples following SHS possess a uniform microstructure with localized regions enriched in the alloying components Nb and Mo, as depicted in Fig. 3. No unreacted Ti and Al particles were detected. An increase in the TiH_2 concentration in the initial mixture resulted in a reduction in the grain size of the synthesis products. This effect is attributed to the intense hydrogen evolution and, consequently, the disruption of the briquettes' integrity, leading to increased porosity in the SHS-sintered samples.

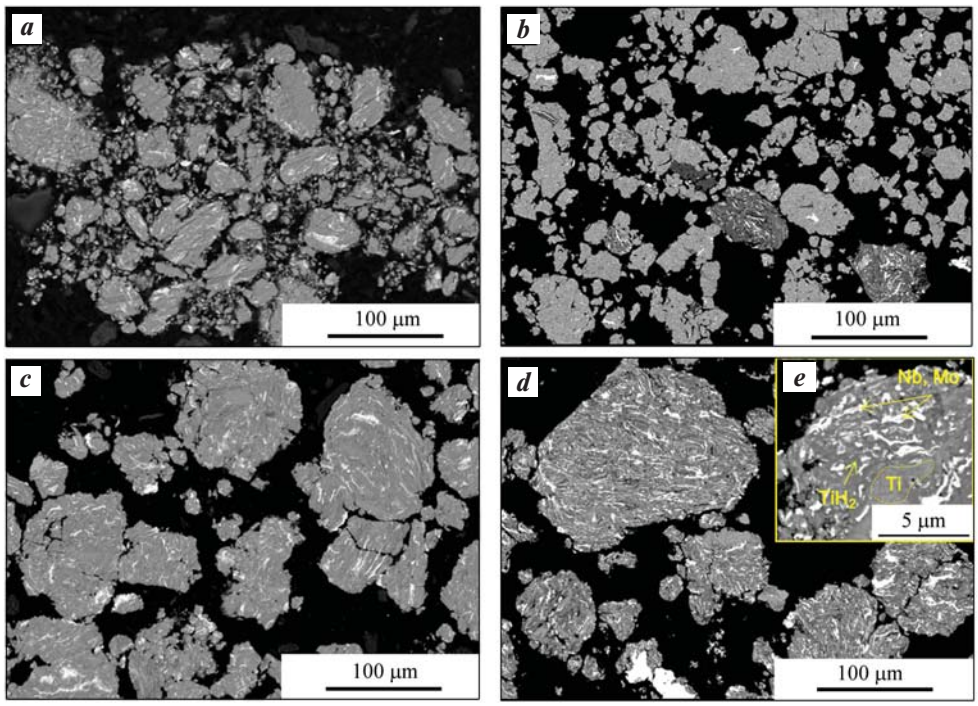

Fig. 1. Structure of Ti/TiH_2–Nb–Mo–B–Y_2O_3 powder particles after HEBM
TiH_2, wt.%: 10 (***a***), 20 (***b***), 30 (***c***), 40 (***d***, ***e***)

Рис. 1. Структура порошковых частиц Ti/TiH_2–Nb–Mo–B–Y_2O_3 после ВЭМО
TiH_2, мас.%: 10 (***a***), 20 (***b***), 30 (***c***), 40 (***d***, ***e***)

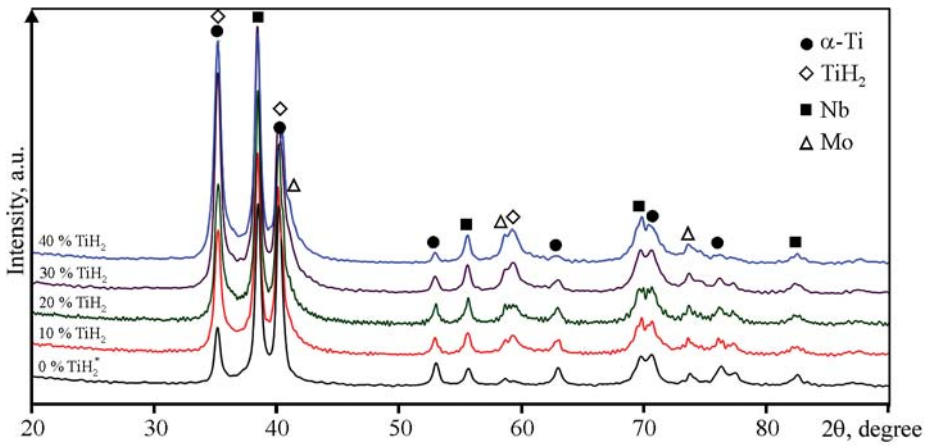

Fig. 2. *X*-ray diffraction patterns of Ti/TiH_2–Nb–Mo–B–Y_2O_3 powders after HEBM
(0%TiH_2 XRD pattern based on the data published in [13])

Рис. 2. Рентгенограммы лигатур Ti/TiH_2–Nb–Mo–B–Y_2O_3 после ВЭМО
(на основе материалов, опубликованных в работе [13])

According to the XRD data (Fig. 4), the resulting SHS powder consists of 78 % γ-TiAl (*P*4/*mmm*), 19 % α_2-Ti_3Al (*P*63/*mmc*), and 3 % solid solution (Nb) (*Im*-3*m*). The absence of TiH_2 peaks suggests that during the SHS process, this phase underwent complete decomposition, and the resulting metallic titanium reacted with aluminum. The formation of γ-TiAl and α_2-Ti_3Al follows a reaction diffusion mechanism. Initially, aluminum melts and spreads over the titanium surface, accompanied by the creation of the $TiAl_3$ phase. As the liquid phase diminishes and diffusion interaction between Ti and $TiAl_3$ becomes active, intermetallic

compounds form in the following sequence: $TiAl_2 \rightarrow$ $\rightarrow TiAl \rightarrow Ti_3Al$ [24—26]. The powder particles obtained via the SHS method exhibit a microgradient structure based on the α_2-Ti_3Al and γ-TiAl phases (Fig. 3).

Compact samples of the TNM-B1+1%Y_2O_3 alloy were produced using the HIP method. To achieve a lamellar microstructure, the alloys were further subjected to HT. The resulting microstructures of the alloy are depicted in Fig. 5. The sample after HIP exhibits a fine-grained globular structure inherited from SHS powders, with the primary structural components taking the form of γ-TiAl and α_2-Ti_3Al phases. Fine aluminum oxide particles are also observable in SEM images, but their concentration in the alloy with 10 % TiH_2 is minimal. *X*-ray diffraction patterns indicate that the intensity of the peaks corresponding to the Al_2O_3 phase

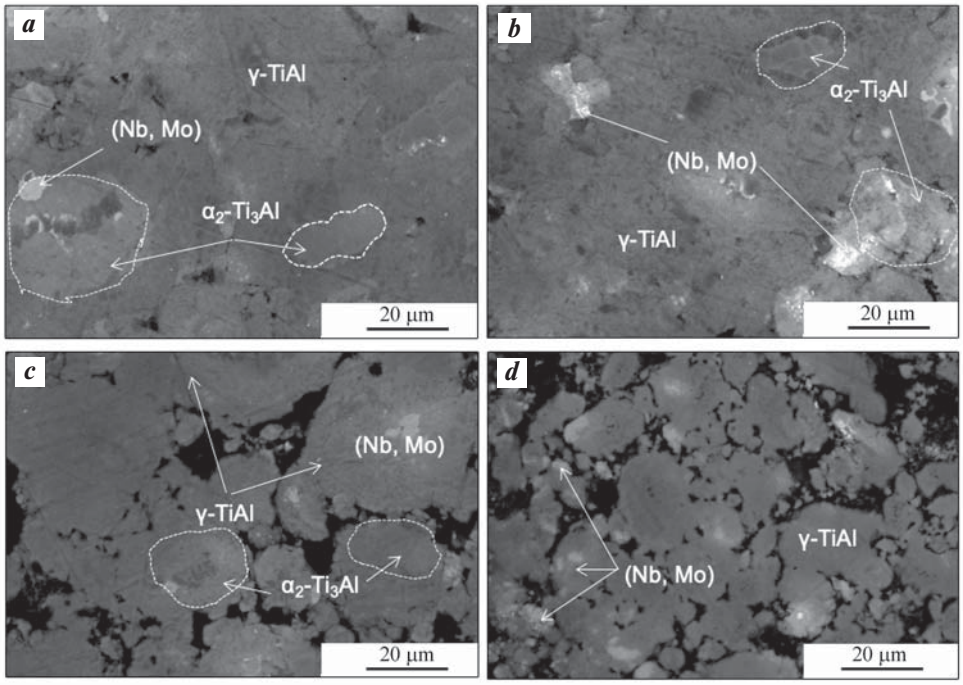

Fig. 3. SHS-sintered samples' structure after the addition of TiH_2 to the reaction mixtures
TiH_2, wt.%: 10 (***a***), 20 (***b***), 30 (***c***), 40 (***d***)

Рис. 3. Структура СВС-спеков, полученных из реакционных смесей с добавлением TiH_2
TiH_2, мас.%: 10 (***a***), 20 (***b***), 30 (***c***), 40 (***d***)

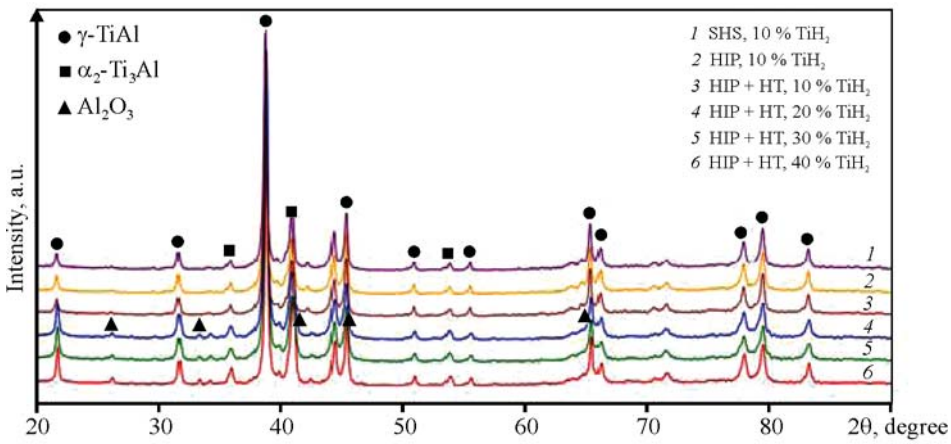

Fig. 4. *X*-ray diffraction patterns of alloy with varying TiH_2 content after SHS, HIP and HIP + HT

Рис. 4. Рентгенограммы сплава с различным содержанием TiH_2 после СВС, ГИП и ГИП + ТО

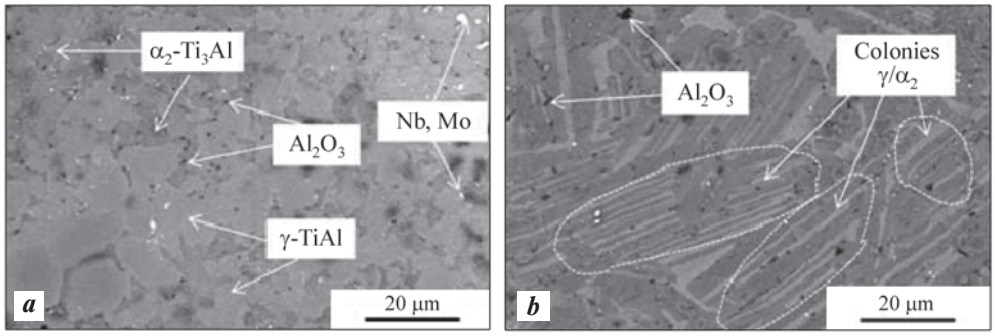

Fig. 5. Structure of the TNM-B1+1%Y_2O_3 alloy with 10% TiH_2 after HIP (***a***) and HIP + HT (***b***)

Рис. 5. Структура сплава TNM-B1+1%Y_2O_3 с 10 % TiH_2 после ГИП (***a***) и ГИП + ТО (***b***)

increases in samples with the addition of 20 % TiH_2 and higher.

Heat treatment of the TNM-B1+1%Y_2O_3 alloy enabled the transformation of its structure from globular to partially lamellar. During heating to 1380 °C, the alloy transitions from the two-phase region (α + γ) of the phase diagram to the single-phase region (α-Ti), where the γ-TiAl phase dissolves and becomes saturated with aluminum. Upon cooling below the eutectoid transformation temperature, the α phase disintegrates into alternating dispersed lamellae of γ-TiAl and α_2-Ti_3Al, forming colonies. In between these colonies, a small portion of equiaxed grains of the γ-TiAl and α_2-Ti_3Al phases remains.

Structure and mechanical properties of TNM-B1+1%Y_2O_3 alloy after HIP and HIP + HT

The microstructures of TNM-B1+1%Y_2O_3 alloy samples after HIP and HIP + HT, which vary in the TiH_2 content in the initial powders, are depicted in Fig. 6. The alloys exhibit the presence of γ-TiAl and α_2-Ti_3Al phases with equiaxed and lamellar structures, respectively. Additionally, a small amount of dispersed solid solution particles (Nb, Mo) can be observed. As the quantity of TiH_2 in the initial powder mixtures increases, there is a tendency for the occurrence and an increase in the content of Al_2O_3. These Al_2O_3 particles are presented in the form of dispersed particles located along the boundaries of the coarse grains of γ-TiAl and α_2-Ti_3Al.

To ascertain the reasons for the formation of Al_2O_3 in compositions with a high TiH_2 concentration as a precursor, the oxygen and nitrogen contents were analyzed after each technological procedure (HEBM, SHS, and HIP). In this experiment, powder mixtures, SHS products, and consolidated samples served as reference samples, prepared using only metallic titanium as the initial material.

It was found that the oxygen concentration after HEBM exhibited a weak dependence on the TiH_2 content and measured at 0.67 %, 0.57 %, 0.59 %, 0.68 %, and 0.65 %, while the nitrogen concentration was 0.049 %, 0.039 %, 0.043 %, 0.046 %, and 0.052 % for compositions with 0 %, 10 %, 20 %, 30 %, and 40 % TiH_2, respectively. The most substantial increase in impurity oxygen was recorded at the SHS stage, rising from 0.8 % to 2.8 % (Fig. 7). Following the HIP stage, the amount of gas impurities remained nearly unchanged.

Regarding the chemical purity of the alloys, the optimal Ti : TiH_2 ratio was found to be 90 : 10 (Fig. 7). The nature of the dependence of impurity oxygen content on the TiH_2 amount in the initial charge can be explained by two competing factors. On one hand, the presence of TiH_2 in the charge creates a localized reducing atmosphere due to the release of hydrogen during its decomposition in the SHS process. On the other hand, as shown earlier, excessive gas evolution leads to increased residual porosity in SHS-sintered products, an increase in the specific surface area of synthesis products, and adsorption.

The impact of TiH_2 content in the reaction mixtures on the mechanical properties of alloys after HIP and HIP + HT was evaluated using strain diagrams depicting “true compressive stress — logarithmic strain” (Fig. 8). The test results (refer to Table 1) demonstrated that the alloy with a Ti : TiH_2 ratio of 90 : 10 exhibited the highest level of strength properties, with σ_u = = 1200±15 MPa and YS = 1030±25 MPa. The reduction in strength and increased brittleness in samples with higher TiH_2 content can be attributed to the embrittling effect of Al_2O_3 particles.

In TNM-B1+1%Y_2O_3 alloys, an improvement in

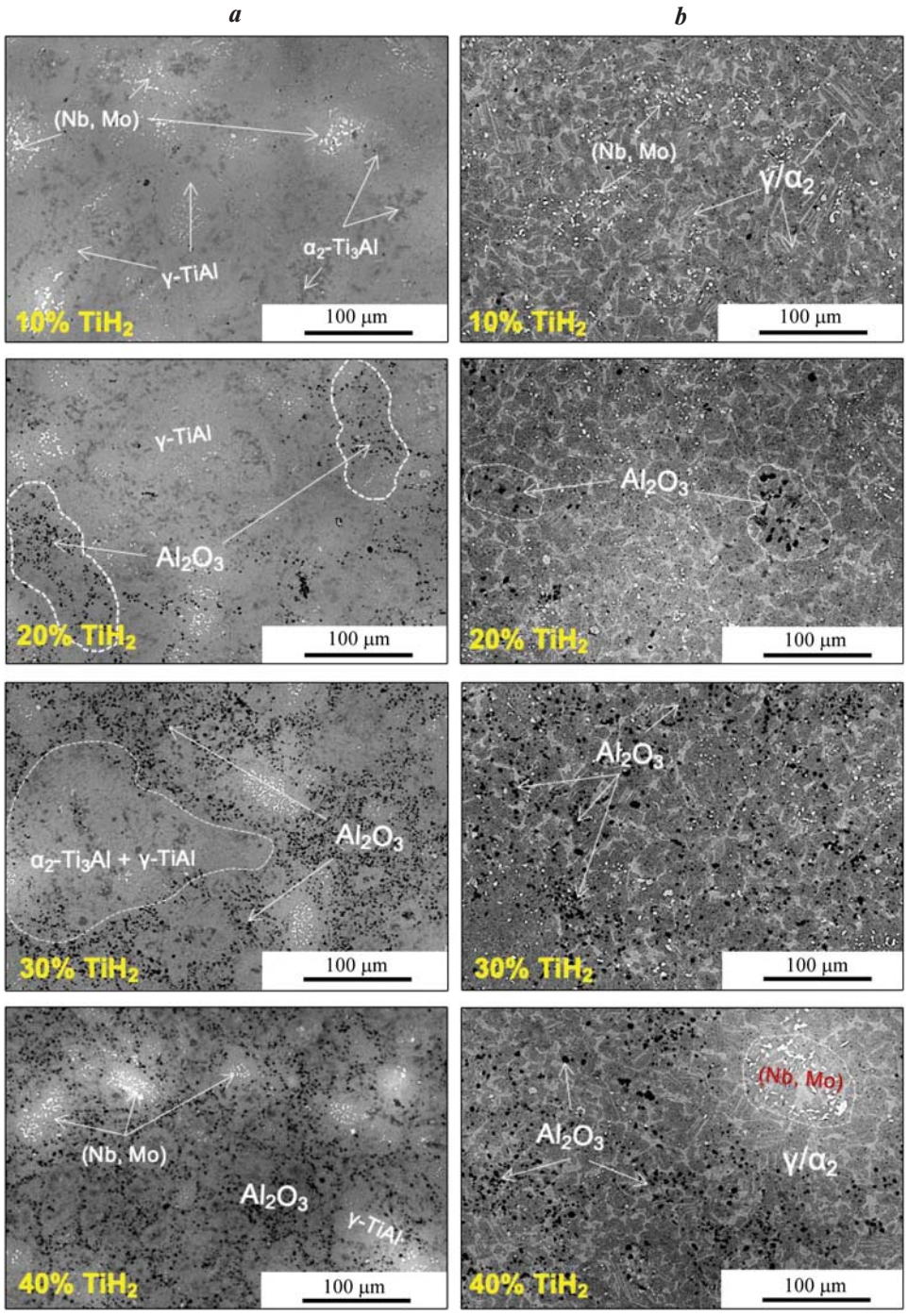

Fig. 6. Structure of the TNM-B1+1%Y_2O_3 alloy after HIP (***a***) and HIP + HT (***b***)

Рис. 6. Структура сплава TNM-B1+1%Y_2O_3 после ГИП (***a***) и ГИП + ТО (***b***)

strength and resistance to plastic deformation was observed after HIP + HT. This can be attributed to the characteristics of the microstructure. The partially lamellar structure results in a decrease in the average size of grains and lamellae inside colonies, from 2.5 to 0.3 μm. This reduction leads to a decrease in the mean free path of dislocations during deformation. Notably, the alloy in which titanium was substituted by its hydride also exhibited the highest strength, with σ_u = = 1253±15 MPa and YS = 1090±30 MPa.

The studied alloys TNM-B1+1%Y_2O_3, both with globular and partially lamellar microstructure, surpassed the classical alloy 4822 [2] and the more intricately doped analogs, Ti—46Al—4Nb—1Mo and Ti—45Al—8.5Nb—0.2W—0.2B [27; 28], in terms of strength.

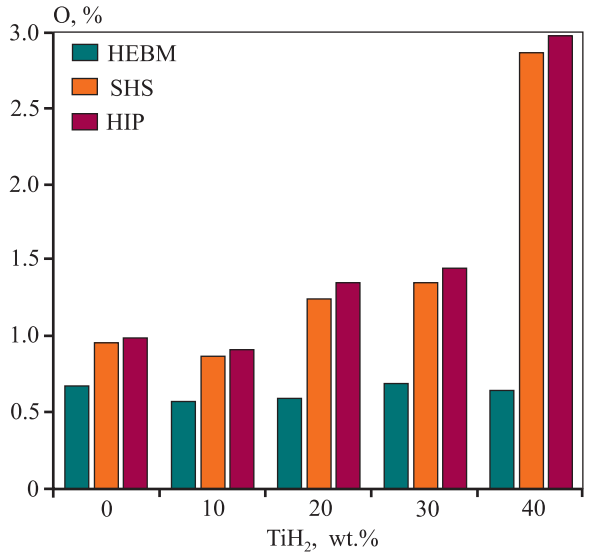

Fig. 7. Content of oxygen impurity in the TNM-B1+1%Y_2O_3 alloy with Ti : TiH_2 varying ratios after HEBM, SHS, and HIP

Рис. 7. Содержание примесного кислорода в сплаве TNM-B1+1%Y_2O_3 с различным соотношением Ti : TiH_2 после ВЭМО, СВС и ГИП

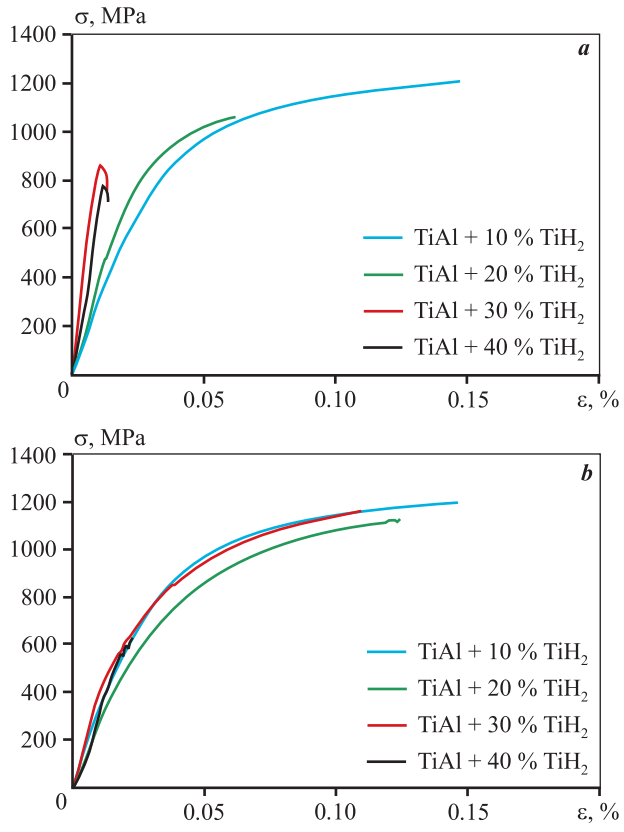

Fig. 8. Stress-strain diagrams for the TNM-B1+1%Y_2O_3 alloy obtained from SHS powders after HIP (***a***) and HIP + HT (***b***)

Рис. 8. Диаграммы логарифмической деформации при сжатии для полученного из СВС-порошков сплава TNM-B1+1%Y_2O_3 после ГИП (***a***) и ГИП + ТО (***b***)

Mechanical properties of the TNM-B1+1%Y_2O_3 alloy compact samples following HIP and HIP + HT

Механические свойства компактных образцов сплава TNM-B1+1%Y_2O_3 после ГИП и ГИП + ТО

Treatment	Content of TiH_2, wt.%	σ_u, MPa	YS, MPa	ε, %
HIP	10	1200±15	1030±25	0.010
	20	1053±50	953±20	0.009
	30	830±45	–	0.007
	40	742±32	–	0.006
HIP + HT	10	1253±15	1090±30	0.010
	20	1122±55	988±25	0.009
	30	1165±58	995±15	0.010
	40	630±25	–	0.005

Conclusions

1. The study investigated the influence of the Ti : TiH_2 ratio in the reaction mixture, along with heat treatment, on the microstructure and mechanical properties of the TNM-B1+1% Y_2O_3 alloy, which was obtained using the HEBM, SHS, and HIP methods. The substitution of 10 % of titanium with its hydride in reaction mixtures led to a reduction in the oxygen content in SHS products from 1.0 % to 0.8 %. This reduction can be attributed to the generation of a reducing atmosphere during the decomposition of TiH_2 in the combustion wave.

2. The maximum mechanical properties of the TNM-B1+1%Y_2O_3 alloy were achieved at a Ti : TiH_2 ratio of 90 : 10, with the compressive strength (σ_u) measuring 1200±15 MPa and YS measuring 1030±25 MPa. However, an increase in the proportion of TiH_2 led to a higher content of oxygen impurity, resulting in the formation of Al_2O_3. This, in turn, reduced the strength and ductility of the material.

3. Heat treatment of the TNM-B1+1%Y_2O_3 alloy transformed the globular structure into a partially lamellar one, resulting in an increase in σ_u by 50—300 MPa, depending on the TiH_2 content. This improvement can be attributed to a reduction in the average grain size and a decrease in dislocation mobility during deformation.

References

1. Burtscher M., Klein T., Lindemann J., Lehmann O., Fellmann H., Güther V., Clemens H., Mayer S. An advanced

TiAl alloy for high-performance racing applications. *Materials*. 2020;13(21):4720. https://doi.org/10.3390/ma13214720

2. Зайцев А.А., Капланский Ю.Ю., Сентюрина Ж.А., Левашов Е.А., Касимцев А.В., Погожев Ю.С., Юдин С.Н., Свиридова Т.А., Маляров А.В. Получение спеченного сплава на основе интерметаллида TiAl. Ч. 2. Исследование процессов формования и спекания. *Известия вузов. Цветная металлургия*. 2016;(1):50—62. https://doi.org/10.17073/0021-3438-2016-1-50-62
Zaitsev A.A., Kaplanskii Y.Y., Sentyurina Z.A., Levashov E.A., Kasimtsev A.V., Pogozhev Y.S., Yudin S.N., Sviridova T.A., Malyarov A.V. Production of a sintered alloy based on the TiAl intermetallic compound: Pt. 2. Investigation into forming and sintering processes. *Russian Journal of Non-Ferrous Metals*. 2016;57:113—123. https://doi.org/10.3103/S1067821216020139
3. Касимцев А.В., Юдин С.Н., Свиридова Т.А., Маляров А.В., Зайцев А.А., Сентюрина Ж.А., Капланский Ю.Ю., Погожев Ю.С., Левашов Е.А. Получение спеченного сплава на основе интерметаллида TiAl. Ч. 1. Гидридно-кальциевая технология получения порошкового сплава Ti—47Al—2Nb—2Cr и его свойства. *Известия вузов. Цветная металлургия*. 2015;(4): 63—68. https://doi.org /10.17073/0021-3438-2015-4-63-68
Kasimtsev A.V., Yudin S.N., Sviridova T.A., Malyarov A.V., Zaitsev A.A., Sentyurina Zh.A., Kaplanskii Yu.Yu., Pogozhev Yu.S., Levashov E.A. Production of a sintered alloy based on the TiAl intermetallic compound. Pt. 1: Calcium-hydride fabrication technology of the Ti—47Al—2Nb—2Cr powder alloy and its properties. *Russian Journal of Non-ferrous Metals*. 2015;56:548—554. https://doi.org/10.3103/S1067821215050065
4. Bewlay B.P., Nag S., Suzuki A., Weimer M.J. TiAl alloys in commercial aircraft engines. *Materials at High Temperatures*. 2016;33(4-5):549—559. https://doi.org/10.1080/09603409.2016.1183068
5. Rittinghaus S.K., Zielinski J. Influence of process conditions on the local solidification and microstructure during laser metal deposition of an intermetallic TiAl alloy (GE4822). *Metallurgical and Materials Transactions: A*. 2021;52:1106—1116. https://doi.org/10.1007/s11661-021-06139-2
6. Ostrovskaya O., Badini C., Deambrosis S.M., Miorin E., Biamino S., Padovano E. Protection from oxidation of second and third generation TiAl intermetallic alloys by magnetron sputtering deposition of a TiAl/TiAlN coating. *Materials & Design*. 2021;208:109905. https://doi.org/10.1016/j.matdes.2021.109905
7. Abdoshahi N., Dehghani M., Hatzenbichler L., Spoerk-Erdely P., Ruban A.V., Musi M., Mayer S., Spitaler J., Holec D. Structural stability and mechanical properties of TiAl + Mo alloys: A comprehensive ab initio study. *Acta Materialia*. 2021; 221:117427. https://doi.org/10.1016/j.actamat.2021.117427
8. Полькин И.С., Гребенюк О.Н., Саленков В.С. Интерметаллиды на основе титана. *Технология легких сплавов*. 2010;2:5—15. https://cyberleninka.ru/article/n/intermetallidy-na-osnove-titana-1 (дата обращения 28.09.2023)
Pol'kin I.S., Grebenyuk O.N., Salenkov V.S. Intermetallic compounds based on titanium. *Tekhnologiya legkikh splavov*. 2010;2:5—15. (In Russ.).
9. Kamyshnykova K., Lapin J. Vacuum induction melting and solidification of TiAl-based alloy in graphite crucibles. *Vacuum*. 2018;154:218—226. https://doi.org/10.1016/j.vacuum.2018.05.017
10. Siheng G., Xianjuan D., Xuan X., Yong X. Effect of ball milling speed and sintering temperature on microstructure and properties of TiAl alloy prepared by powder metallurgy. *Procedia Manufacturing*. 2020;50:355—361. https://doi.org/10.1016/j.promfg.2020.08.066
11. Knörlein J., Franke M.M., Schloffer M., Berger T., Körner C. Microstructure and mechanical properties of additively manufactured γ-TiAl with dual microstructure. *Intermetallics*. 2023;161:107978. https://doi.org/10.1016/j.intermet.2023.107978
12. Wu X. Review of alloy and process development of TiAl alloys. *Intermetallics*. 2006;14(10-11):1114—1122. https://doi.org/10.1016/j.intermet.2005.10.019
13. Loginov P.A., Kaplanskii Y.Y., Markov G.M., Patsera E.I., Vorotilo K.V., Korotitskiy A.V., Shvyndina N.V., Levashov E.A. Structural and mechanical properties of Ti—Al—Nb—Mo—B alloy produced from the SHS powder subjected to high-energy ball milling. *Materials Science and Engineering: A*. 2021;814:141153. https://doi.org/10.1016/j.msea.2021.141153
14. Taguchi K., Ayada M., Ishihara K.N., Shingu P.H. Near-net shape processing of TiAl intermetallic compounds via pseudoHIP-SHS route. *Intermetallics*. 1995;3(2):91—98. https://doi.org/10.1016/0966-9795(95)92673-N
15. Aguilar J., Schievenbusch A., Kättlitz O. Investment casting technology for production of TiAl low pressure turbine blades—Process engineering and parameter analysis. *Intermetallics*. 2011;19(6):757—761. https://doi.org/10.1016/j.intermet.2010.11.014
16. Lagos M.A., Agote I. SPS synthesis and consolidation of TiAl alloys from elemental powders: Microstructure evolution. *Intermetallics*. 2013;36:51—56. https://doi.org/10.1016/j.intermet.2013.01.006
17. Бусурина М.Л., Умаров Л.М., Ковалев И.Д., Сачкова Н.В., Бусурин С.М., Вадченко С.Г., Сычев А.Е. Особенности структуро- и фазообразования в системе

Ti—Al—Nb в режиме теплового взрыва. *Физика горения и взрыва*. 2016;52(6):44—50. https://doi.org/10.1134/S0010508216060058
Busurina M.L., Umarov L.M., Kovalev I.D., Sachkova N.V., Busurin S.M., Vadchenko S.G., Sychev A.E. Features of structure and phase formation in the Ti—Al—Nb system in the thermal explosion mode. *Combustion, Explosion and Shock Waves*. 2016;52(6): 659—664. https://doi.org/10.15372/FGV20160605
18. Mukasyan A.S., Rogachev A.S. Combustion behavior of nanocomposite energetic materials. *Energetic Nanomaterials*. 2016;163—192. https://doi.org/10.1016/B978-0-12-802710-3.00008-8
19. Rak Z.S., Walter J. Porous titanium foil by tape casting technique. *Journal of materials processing technology*. 2006;175(1-3):358—363. https://doi.org/10.1016/j.jmatprotec.2005.04.066
20. Bidaux J.E., García-Gómez J., Hamdan H., Zufferey D., Rodríguez-Arbaizar M., Girard H., Carreno-Morelli E. Tape casting of porous titanium thin sheets from titanium hydride. In: *Proceedings of the Euro PM2011 Congress & Exhibition*. (Barcelona, Spain. 9—12 October 2011). 2011. P. 2.
21. Samal S., Cho S., Park D.W., Kim H. Thermal characterization of titanium hydride in thermal oxidation process. *Thermochimica Acta*. 2012;542:46—51. https://doi.org/10.1016/j.tca.2012.02.010
22. Peillon N., Fruhauf J.B., Gourdet S., Feraille J., Saunier S., Desrayaud C. Effect of TiH_2 in the preparation of MMC Ti based with TiC reinforcement. *Journal of Alloys and Compounds*. 2015; 619:157—164. https://doi.org/10.1016/j.jallcom.2014.09.014
23. Azevedo C.R.F., Rodrigues D., Neto F.B. Ti—Al—V powder metallurgy (PM) via the hydrogenation-dehydrogenation (HDH) process. *Journal of Alloys and Compounds*. 2003;353(1-2):217—227. https://doi.org/10.1016/S0925-8388(02)01297-5
24. Курбаткина В.В., Пацера Е.И., Бодян А.Г., Левашов Е.А. Получение субмикронного порошка на основе TiAl в режиме теплового взрыва. *Цветные металлы*. 2017;2:68—73. https://doi.org/10.17580/tsm.2017.02.11
Kurbatkina V.V., Patsera E.I., Bodyan A.G., Levashov E.A. Preparation of submicron TiAl-based powder in thermal explosion mode. *Tsvetnye metally*. 2017;2:68—73. (In Russ.). https://doi.org/10.17580/tsm.2017.02.11
25. Xu W.C., Huang K., Wu S.F., Zong Y.Y., Shan D.B. Influence of Mo content on microstructure and mechanical properties of β-containing TiAl alloy. *Transactions of Nonferrous Metals Society of China*. 2017;27(4):820—828. https://doi.org/10.1016/S1003-6326(17)60094-3
26. Pan Y., Lu X., Liu C., Hui T., Zhang C., Qu X. Sintering densification, microstructure and mechanical properties of Sn-doped high Nb-containing TiAl alloys fabricated by pressureless sintering. *Intermetallics*. 2020;125:106891. https://doi.org/10.1016/j.intermet.2020.106891
27. Li Z., Luo L., Su Y., Wang B., Wang L., Liu T., Yao M., Liu C., Guo J., Fu H. A high-withdrawing-rate method to control the orientation of $(\gamma + \alpha_2)$ lamellar structure in a β-solidifying γ-TiAl-based alloy. *Materials Science and Engineering: A*. 2020;857:144078. https://doi.org/10.1016/j.msea.2022.144078
28. Qiang F., Kou H., Tang B., Song L., Li J. Effect of cooling rate on microstructure evolution of Ti—45Al—8.5—Nb0.2—W0.2—B0.02—Y alloy during multi-step heat treatment. *Materials Characterization*. 2018;145:210—217. https://doi.org/10.1016/j.matchar.2018.08.031

Information about the authors

Georgy M. Markov – Junior Research Scientist of the "In situ Diagnostics of Structural Transformations" Laboratory of Scientific Educational Center of Self Propagating High-Temperature Synthesis (SEC SHS), MISIS–ISMAN, National University of Science and Technology (NUST) "MISIS".
https://orcid.org/0000-0001-7285-7888
E-mail: markov.sci@gmail.com

Pavel A. Loginov – Cand. Sci. (Eng.), Senior Research Scientist of the "In situ Diagnostics of Structural Transformations" Laboratory of SEC SHS, MISIS–ISMAN.
https://orcid.org/0000-0003-2505-2918
E-mail: pavel.loginov.misis@list.ru

Nataliya V. Shvyndina – Leading Engineer of SEC SHS, MISIS–ISMAN.
https://orcid.org/0000-0002-4662-544X
E-mail: natali19-03@list.ru

Информация об авторах

Георгий Михайлович Марков – мл. науч. сотрудник лаборатории «In situ диагностика структурных превращений» научно-учебного центра (НУЦ) СВС, МИСИС–ИСМАН, Национальный исследовательский технологический университет (НИТУ) «МИСИС».
https://orcid.org/0000-0001-7285-7888
E-mail: markov.sci@gmail.com

Павел Александрович Логинов – к.т.н., ст. науч. сотрудник лаборатории «In situ диагностика структурных превращений» НУЦ СВС, МИСИС–ИСМАН.
https://orcid.org/0000-0003-2505-2918
E-mail: pavel.loginov.misis@list.ru

Наталия Владимировна Швындина – вед. инженер НУЦ СВС, МИСИС–ИСМАН.
https://orcid.org/0000-0002-4662-544X
E-mail: natali19-03@list.ru

Fedor A. Baskov – Cand. Sci. (Eng.), Research Scientist of the "In situ Diagnostics of Structural Transformations" Laboratory of SEC SHS, MISIS–ISMAN, Head of Sector, JSC "Composite".
https://orcid.org/0000-0001-6238-4378
E-mail: baskov_fa@mail.ru

Evgeny A. Levashov – Dr. Sci. (Eng.), Professor, Full Member of Russian Academy of Natural Science, Head of Department of Powder Metallurgy and Functional Coatings, NUST "MISIS", Head of SEC SHS, MISIS–ISMAN.
https://orcid.org/0000-0002-0623-0013
E-mail: levashov@shs.misis.ru

Федор Алексеевич Басков – к.т.н., науч. сотрудник лаборатории «In situ диагностика структурных превращений» НУЦ СВС, МИСИС–ИСМАН, начальник сектора АО «Композит».
https://orcid.org/0000-0001-6238-4378
E-mail: baskov_fa@mail.ru

Евгений Александрович Левашов – д.т.н., проф., академик РАЕН, академик Всемирной академии керамики, зав. кафедрой порошковой металлургии и функциональных покрытий НИТУ «МИСИС», директор НУЦ СВС, МИСИС–ИСМАН.
https://orcid.org/0000-0002-0623-0013
E-mail: levashov@shs.misis.ru

Contribution of the authors

Georgy M. Markov – formulated the research purpose, prepared initial materials, conducted experiments, and wrote the manuscript.

Pavel A. Loginov– formulated the research purpose, participated in result discussions, and reviewed and edited the article.

Natalia V. Shvyndina – conducted microscopy examinations and participated in result discussions.

Fedor A. Baskov – carried out sample compaction and participated in result discussions.

Evgeniy A. Levashov – contributed to the conceptualization and supervised the article, participated in result discussions.

Вклад авторов

Г.М. Марков – определение цели работы, подготовка исходных материалов, проведение экспериментов, написание текста статьи.

П.А. Логинов – определение цели работы, участие в обсуждении результатов, проведение обзора и редактирование статьи.

Н.В. Швындина – проведение микроскопических исследований, участие в обсуждении результатов.

Ф.А. Басков – проведение компактирования образцов, участие в обсуждении результатов.

Е.А. Левашов – концептуализация и проверка статьи, участие в обсуждении результатов.

The article was submitted 28.09.2023, revised 11.10.2023, accepted for publication 13.10.2023

Статья поступила в редакцию 28.09.2023, доработана 11.10.2023, подписана в печать 13.10.2023